Technical Journal, University of Engineering and Technology (UET) Taxila, Pakistan Vol. 23 No. 4-2018
ISSN:1813-1786 (Print) 2313-7770 (Online)

Performance of T-joints repaired with different CFRP arrangements

M. F. Tahir[1], S. Mehboob[2], Q. U. Z. Khan[3], F. Shabir[4]

[1,2,3,4]*Civil Engineering Department, University of Engineering & Technology, Taxila, Pakistan*
[1]fiaz.tahir@uettaxila.edu.pk

Abstract-In this investigation, carbon fiber reinforced polymers (CFRP) were used for repairing of six damaged reinforced concrete (RC) beam-column T joints. Two different types of CFRP configurations (1 & 2) were employed to reinstate the seismic capacity of joints. The specimens were tested under cyclic axial loading till failure. Load deflection relationships of tested specimens were used to draw hysteresis loops and backbone curves. In order to assess the seismic performance this data was then used to calculate energy dissipation values at selected intervals. Finite element modelling of all three types was also done in ANSYS to validate model. It was concluded that seismic capacity of repaired specimen is affected by CFRP configuration techniques. It was found that the relative energy dissipation capacity of specimens repaired with CFRP configuration-2 was 25.43% higher than CFRP configuration-1.Cumulative energy dissipation capacity was 5.24% higher in CFRP configuration-2 as compared to CFRP configuration-1. It was also found that the prevailing cracking pattern of repaired columns largely affects response of repaired specimen. Study also concluded that performance of Beam-column joints can be improved by appropriately selecting CFRP configuration without altering other parameters.

Keywords-Beam-Column Joint, CFRP Configuration, Energy Dissipation, Reinforced Concrete, ANSYS.

I. INTRODUCTION

Carbon fiber reinforced polymers (CFRP) can be used for repairing of RC structural elements with following deficiencies [i]: Inadequate reinforcement detailing, steel quantity less than desired as per structural drawings, concrete having strength lesser than specified, development of cracks due to seismic activity and over loads change in the use of structures.

Advantages of fiber reinforced polymers (FRP) include high strength, easy installation procedure, light weight and immunity to corrosion [ii]. Further, in FRP repaired members, there is no significant increase in member size [iii]. All types of members like beams, columns and slabs are successfully being retrofitted and repaired since the introduction of FRP. For example, [iv] examined the efficiency of external strengthening systems for RC beams using FRP fabric (Glass–Carbon). While [v] used CFRP wraps to repair low strength concrete columns. It was observed [vi], a 35% increase in shear capacity of joints. Researchers [vii] used FRP to strengthen slab column connections and observed 29% increase in punching capacity and 80% increase in stiffness. Author [viii] repaired beam column joints with two different configurations of CFRP laminates and found improvement in ultimate strength and deflection. However, for the laminate configurations stiffness was decreased.

It is pertinent to discuss here that despite specific in location on structural members, the seismic damage of specimen is not uniform due to nature of loading, internal micro structures of concrete and arrangement of reinforcement. The efficiency of CFRP repairing is also affected by nature of damage. Further, the overall performance of repaired or retrofitted members is also affected by repairing methodology adopted.

In [ix] described various steps adopted in repairing of beam, column joints with CFRP. According to [x] first step is the removal of loose or crushed concrete. Next step is repairing of existing cracks by epoxy injection [xi]. Epoxy injection is a very careful process and is sensitive to many factors. Especially, if outer sides of cracks are not properly sealed from outside, epoxy may not reach its proper location. Application pressure of epoxy is also important. However, if cracks are not too large and concrete is not crushed, epoxy can be injected without removal of concrete [xii, xiii]. If concrete is severely damaged, concrete in the entire region can be removed and replaced with high strength and low or no-shrink grout [ix].

Proper bond between CFRP and concrete surface ensures composite action by developing stress transfer between beam and column. Bond strength is affected by factors like bonded length, concrete strength, number of plies, ply width and surface preparation. It has been observed that bond strength increases with the increase in compressive strength of concrete. However, bond length of CFRP sheet has minimal effect [xiv]. It has been found that stiffness of fiber sheets also increases ultimate load capacity of the repaired sheets [xv].

Strength and ductility are important physiognomies of beam column joints endangered to seismic demand. A part of seismic input energy imparted to a structure is dissipated, which culminates by hysteretic action of the structural elements and other non-yielding mechanisms [xvi].

Seismic resistance of structure is improved if its energy dissipation capacity is greater than the input energy in form of seismic waves [xvii, xviii]. Resistance of structure to damage or collapse due to inelastic behavior is expressed in terms of its energy dissipation capacity. Deformable structures offer better resistance to collapse under seismic event as compared to brittle structures.

Deformability is representative parameter of seismic resistance of a structure and is expressed in terms of product of force and deformation [xvii]. Large material deformations such as those required in building components to perform in a ductile manner, are often associated with cracking and degradation of its strength, particularly in concrete structures [xix]. The Performance level of damaged structures can be enhanced by repairing and retrofitting with CFRP. Mechanical connections were investigated both experimentally and numerically. The authors have prepared numerical models on microscopic level in order to get the real-world behavior [xx]. Brittle failure prediction of RC beam-column joint was investigated for the existing structures and an algorithm has been developed in order to reflect the nonlinear shear response of beam-column joint [xxi].

In the present investigation performance of CFRP, repaired beam column joints were evaluated by comparing their energy dissipation capacities. In first phase, six seismically detailed beam column reinforced concrete joints were subjected to quasi-static monotonic loading. These tested specimens were repaired with two different configurations of CFRP laminates. These repaired specimens were than subjected to quasi-static monotonic loading again. It was found that seismic capacity of repaired specimen depends on the CFRP configuration techniques. Relative energy dissipation capacity of specimen repaired with CFRP configuration-2 was 25.43% higher than CFRP configuration-1 at last cycles. Finite element analysis was also performed for all the three types of specimens to endorse experimental work.

II. Methodology

Experimentation was performed in two phases [viii]. In the first phase, seismically detailed beam-column joints were cast and tested under quasi-static monotonic loading. In the second phase specimens were repaired with two different configurations of CFRP laminates and tested again.

III. Testing protocol

This section discusses the member dimensions, reinforcement details and experiment protocol.

A. Specimen Construction

In all specimens, beam and column cross-sectional dimensions were same and kept equal to 200×250mm. Length of column was 800mm and cantilever length of beam beyond column face was 800mm. These dimensions were selected due to limitation of available testing facility while similar cross-sections situation is representing one of the popular field conditions in double story construction. It is sometimes required for architectural reasons. Reinforcement in all specimen was provided as per seismic detailing guidelines of ACI detailing manual 2004 [xxii, xxiii]. Column and beam portions of all joints were confined with closely spaced, 135° seismic stirrups. Longitudinal reinforcement in column and beam was provided with 90° hooks at ends to prevent bar slip. Geometric dimensions and structural details of all specimens were remained same as presented by Tahir [viii] in his work.

Compressive strength of concrete in original specimens was as high as 31MPa when testing was started. Aggregate size was limited to 9.5mm to ensure proper concrete placement in expected congestion areas. Specific gravity of coarse aggregates, fine aggregates and cement was respectively 2.67, 2.71 and 3.15 determined as per ASTM-C-127. Cement, sand and coarse aggregates were mixed in a ratio of 1:1.25:2.5 by weight. Water cement ratio was maintained at 0.45.

B. Test Setup

An illustration of test setup and target load history during the experiments used is explained in detail in previous work [viii].

Although test setup was limited to available laboratory facilities however efforts were aimed at devising a test protocol to obtain reliable data depicting representative member behaviour. The experimentation was performed using a reaction frame, jacks, load cells and deflection gauges.

All specimens were subjected to quasi-static cyclic axial load twice: firstly, in undamaged condition and secondly after retrofitting. In each case a uniform axial load was applied on RC column portion of joint with the help of a jack to keep specimen in position. Loading rate on beam was maintained at 5-10kN/min in accordance with the loading recommended by Mahmoud [i]. This loading was preferred to avoid inertia effects and was measured using a load cell.

C. Failure of Control Specimens

In all control specimen, cracks appeared on tension face of beam. No bar slip phenomena was observed during the test. The test was stopped when beam ceased taking further load.

In control specimen, cracks appeared very close to the column face. However, in repaired specimens, cracks shifted 375mm to 500mm from column face. Fig's. 1-6, show the condition of specimen at the end of test.

D. CFRP Strengthening Details

Specimens tested in first phase were repaired to improve their lost strength. Two different types of CFRP configurations were employed and arranged to improve the flexural capacity joints. CFRP wraps were impregnated with epoxy Chemdur-300. Properties of CFRP and resin used in this research are shown in Table 1.

TABLE 1
MECHANICAL PROPERTIES OF CFRP [viii]

Dry fiber properties	
Tensile Strength(nominal)	4900 N/mm^2
Tensile E-modulus	230.0 N/mm^2
Elongation at break	1.5%
Laminate properties	
Ultimate load	1000 kN/mm^2 (1.4mm thick)
Tensile E-modulus	48.0 kN/mm^2 (1.4mm thick)

Fig. 1. Control specimen 1 after test

Fig. 2. Control specimen 2 after test

Details of CFRP wrap arrangement was selected to provide a required level of resistance against lateral loading in terms of flexure [viii]. In CFRP configuration 2 an additional strip was applied on both faces of beam perpendicular to the crack propagation direction. Specimens repaired with configuration 1 were designated as B-1, B-2 and B-3 whereas repaired with configuration 2 were designated as B-4, B-5 and B-6. During repairing process all cracks were widened using a cutter. The groves thus made were than filled with epoxy Chemdur-300. These treated specimens were than strengthened with CFRP laminates by epoxy. A repaired specimen is shown in Fig. 7.

Fig. 3. Control specimen 3 after test

E. Test results

In the present investigation two types of CFRP configurations were employed for repairing seismically detailed RC beam column joints. Repaired specimens were then again subjected to quasi-static cyclic loads.

Fig. 4. Control specimen 4 after test

ISSN:1813-1786 (Print) 2313-7770 (Online)

Fig. 5. Control specimen 5 after test

Fig. 6. Control specimen 6 after test

Hysteresis loops for all the specimen are shown in Fig's 8-13.

Fig. 7.Specimen strengthened with CFRP laminates

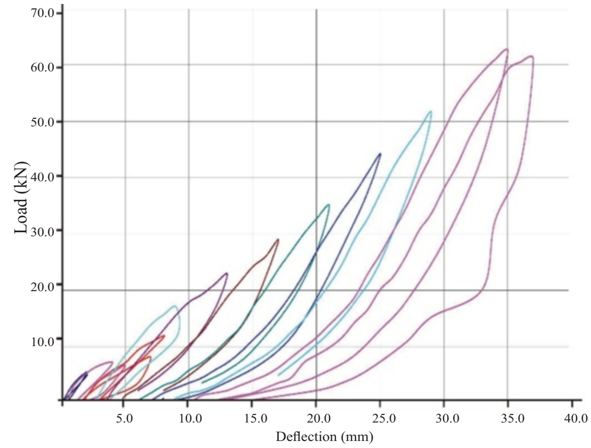

Fig. 8. Hysteresis loop B-1 repaired with CFRP configuration-1

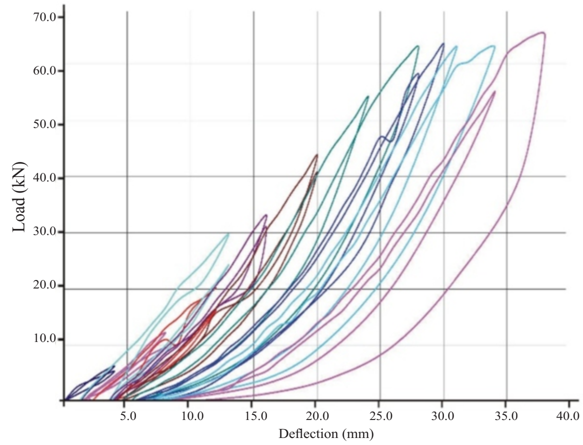

Fig. 9. Hysteresis loop B-2 repaired with CFRP configuration-1

Summary of test results for each specimen is shown in Table II. Similarly, for each specimen and configuration, the data was obtained and summarized in Table III against their average values to facilitate comparison.

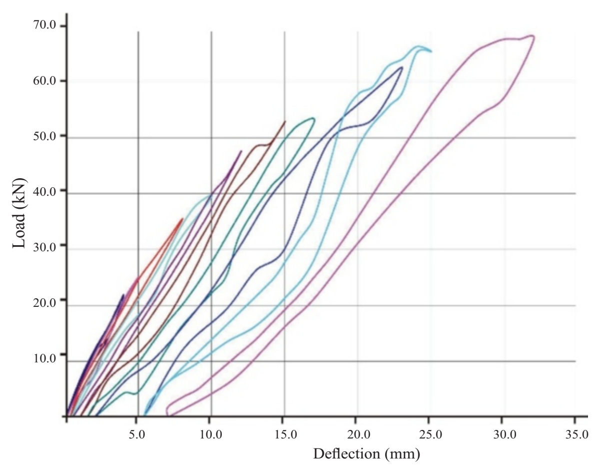

Fig. 10. Hysteresis loop B-3 repaired with CFRP configuration-1

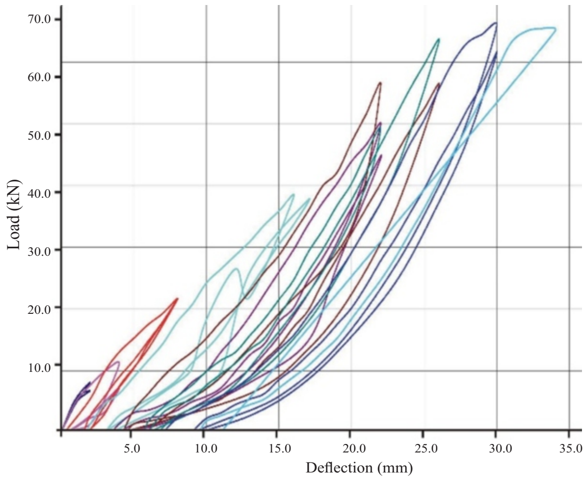

Fig. 11. Hysteresis loop B-4 repaired with CFRP configuration-2

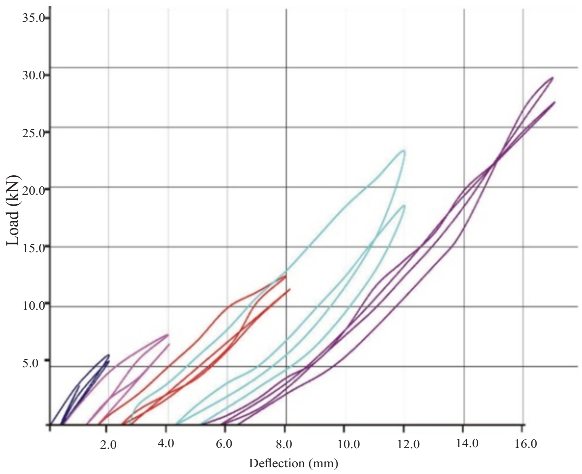

Fig. 12. Hysteresis loop B-5 repaired with CFRP configuration-2

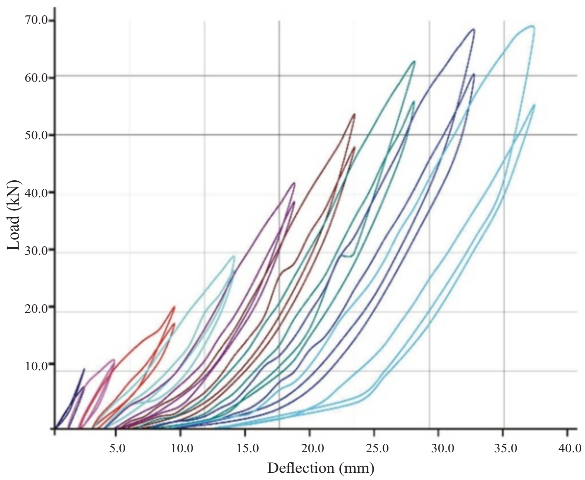

Fig. 13. Hysteresis loop B-6 repaired with CFRP configuration-2

The detail presented in Table II for relative and cumulative energy dissipations capacities were calculated from the hysteresis loops shown in Fig's 8-13. Cumulative energy dissipation capacity for each specimen at each stage was calculated by adding the values determined in present cycle and the values obtained in the previous cycle. Stiffness factor given in the Table II was calculated by taking the ratio of load and relevant deflection.

Response in terms of maximum load, corresponding deflection, energy dissipations and stiffness has been presented in this table for each group individually to depict the overall behaviour of a group. Secant stiffness-based design of RC structures incorporate the secant stiffness in calculations and is defined as the ratio of the strength to the corresponding maximum displacements. Secant Stiffness of the control specimens was 35.87 percent higher than specimens repaired with configuration 1 and 2. It is clear indication that in repaired specimens should be redesigned based on reduced secant stiffness. It was also noted that observed maximum deflection in specimens repaired with configuration 1 and 2 was 71.41 percent higher than the control specimen. Relative energy dissipation capacity at peak load for configuration 2 was 25.43 percent higher than the specimen with configuration 1. However cumulative energy dissipations were only 5.25 percent higher.

IV. ANALYTICAL MODELLING

In this investigation ANSYS software was used for pre-processing and post-processing analysis of all types of specimens.

In the ANSYS pre-processor, the geometry of the beam column joint was built as explained earlier in this paper. Cross sectional dimensions and reinforcement details of specimen modelled in ANSYS is summarized in Table IV.

TABLE II
ANALYSIS OF TEST RESULTS FOR EACH SPECIMEN REPAIRED WITH CFRP

Specimen	Cycle No	Max Load (kN)	Max Deflection (mm)	Relative Energy Dissipation Capacity	Cumulative Energy Dissipation Capacity	Stiffness Factor
B-1 repaired with CFRP configuration-1	0	0.00	0.00	0.000	0	0.000
	1	5.38	2.00	1.120	1.120	2.688
	2	7.17	4.00	7.885	9.005	1.792
	3	9.05	6.00	13.458	22.463	1.508
	4	28.67	17.00	58.912	81.375	1.687
	5	43.90	25.00	74.220	155.595	1.756
	6	51.52	29.00	120.915	276.510	1.777
B-2 repaired with CFRP configuration-1	0	0.00	0.00	0.000	0	0.000
	1	6.27	4.00	3.568	3.568	1.568
	2	12.10	8.00	5.455	9.023	1.512
	3	32.00	16.00	30.299	39.322	2.000
	4	53.76	24.00	50.249	89.571	2.240
	5	62.70	31.00	120.176	209.747	2.023
B-3 repaired with CFRP configuration-1	0	0.000	0.000	0.000	0.000	0.000
	1	21.952	4.000	4.325	4.325	5.488
	2	35.392	8.000	12.327	16.652	4.424
	3	52.864	17.000	64.262	80.914	3.110
	4	66.304	24.000	68.350	149.264	2.763
	5	67.648	30.000	144.519	293.783	2.255
B-4 repaired with CFRP configuration-2	0	0.000	0	0.000	0	0.000
	1	8.064	2	0.622	0.622	4.032
	2	11.200	4	15.360	15.982	2.800
	3	21.504	8	27.870	43.852	2.688
	4	38.080	16	81.153	125.005	2.380
	6	56.000	26	88.704	213.709	2.154
B-5 repaired with CFRP configuration-2	0	0.000	0	0.000	0	0.000
	1	5.824	2	1.778	1.778	2.912
	2	7.616	4	4.605	6.383	1.904
	3	12.544	8	12.212	18.595	1.568
	5	29.120	17	19.880	38.475	1.713
	7	46.592	25	97.440	135.915	1.864
	8	52.864	29	103.300	239.215	1.823
B-6 repaired with CFRP configuration-2	0	0.000	0	0.000	0.000	0.000
	1	7.168	2	0.787	0.787	3.584
	2	11.648	4	7.890	8.677	2.912
	3	20.608	8	20.647	29.324	2.576
	5	41.216	16	51.950	81.274	2.576
	7	61.824	24	103.750	185.024	2.576
	9	67.648	32	183.000	368.024	2.114

TABLE III
COMPARISON OF RESULTS

	Average for config. 1	Average for config. 2	Average for original specimen
Max. Load (kN)	60.62	58.84	54.00
Max. Deflection (mm)	30.00	29.00	17.21
Relative Energy Dissipation	128.54	161.23	-
Cumulative Energy Dissipation	260.01	273.65	-
Stiffness Factor	2.02	2.03	3.15

TABLE IV
INPUT VALUES FOR BEAM-COLUMN JOINT

Parameter	ANSYS Model
Beam	
L×W×D (mm)	800×200×250
Dia. of flexural reinforcement	3-12 mm (#4)
Dia. of hanger bars	2-10 mm (#3)
Stirrups (Ø10 mm) spacing	63 mm c/c
Column	
L×W×D (mm)	800×200×250
Dia. of flexural reinforcement	4-20 mm (#6)
Ties (Ø10 mm) spacing	63 mm c/c

Various elements are available in ANSYS for modelling of different heterogeneous and homogeneous materials composites like concrete, discrete reinforcement, and composites like CFRP. Selection of those constitutive models from the library of ANSYS chiefly depends on the desired results and hence can be utilized in various ways to simulate materials for desired structural behaviour. Three types of materials concrete, steel and CFRP were used in modelling which are discretely described in the following sections, In the simulation, modelling of the concrete was achieved using SOLID65 (8-noded) brick element and the BEAM188 (2-noded) element is selected for the modelling of reinforcement. CFRP was modelled using SOLID46 element.

F. Concrete

Concrete compression strength used was 31MPa. ACI 318-08 [xxii] guidelines were followed to calculate the concrete modulus of elasticity from $E_c = 4700\sqrt{f'_c}$ and concrete cracking stress or rupture module was taken as $f_r = 7.5\lambda\sqrt{f'_c}$ (psi) where $1 = 1$ for normal concrete. The Poisson's ratio for concrete was considered as ν = 0.2. The ANSYS program requires material inputs to capture the behaviour of model already tested experimentally in the laboratory. The uniaxial stress-strain relationship for concrete in compression is a prime requirement for proper formation of concrete material. The mathematical relations; Eq. 1-2, were used besides Eq. 3 to build the stress-strain curve for concrete in this study[xxiv, xxv].

$$f = \frac{E_c \varepsilon}{1 + \left[\frac{\varepsilon}{\varepsilon_o}\right]^2} \tag{1}$$

$$\varepsilon_o = \frac{2f'_c}{E_c} \tag{2}$$

$$E_c = \frac{f}{\varepsilon} \tag{3}$$

Uniaxial crushing stress based on unconfined compressive strength was put as -1 to avoid crushing of concrete. Shear transfer coefficient, βt was used to represent the crack condition in terms of its smoothness and roughness at the face of crack. Its typical value ranges between 0.0 and 1.0 with zero and 1.0 representing smooth and rough crack respectively. The work [xxvi] was used as basis to determine shear transfer coefficient. The values 0.25 and 0.6 of shear transfer coefficient are finally selected after number of trails to account with the convergence problems for non-linear analysis for an open and closed crack respectively in the present study.

G. Steel and CFRP

Yield stress and modulus of elasticity of reinforcement were 414MPa and 200GPa, respectively. The Poisson's ratio "ν" was taken equal to 0.3. It is further assumed that steel behaves in an elastic perfectly plastic manner and the strain hardening modulus is used as 20MPa to avoid loss of stability upon yielding [xxvi]. The material properties used in modelling are summarized in Table V.

TABLE V
SUMMARY OF MATERIAL PROPERTIES USED IN ANSYS

*Material Properties	Values (SI Units)
Concrete	
Density	2400 kg/m^3
Poison's Ratio	0.2
Modulus of Elasticity	26351.6 Mpa
Open Shear Transfer Co-efficient	0.25
Close Shear Transfer Co-efficient	0.6
Ultimate tensile cracking stress	3.467 Mpa
Steel	
Density	7850 kg/m^3
Poison's Ratio	0.3
Modulus of Elasticity	200,000 MPa
Yield Stress	414 MPa
CFRP	
Poison's Ratio	0.22
Modulus of Elasticity	48,000 Mpa
Tensile Strength	10,000 Mpa
Thickness	1.4 mm

*[viii]

H. Numerical Results

After specifying the boundary condition in the pre-processor, control model, model strengthened with CFRP layers of configuration type-1 and model strengthened with CFRP layers of configuration type-2 were analysed and load-deflection plots in the post analysis time-history phase of the ANSYS were generated. The analytical results for control specimen are shown in Fig. 14 and 15.

Fig. 14 and 15 show the deflected shape and crack pattern for control specimen, respectively.

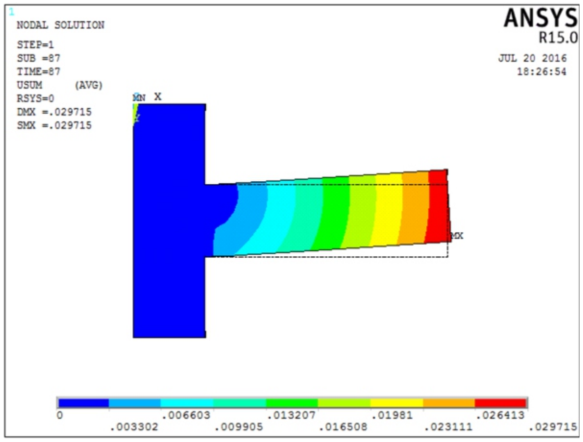

Fig. 14. Control BCJ deflection without CFRP

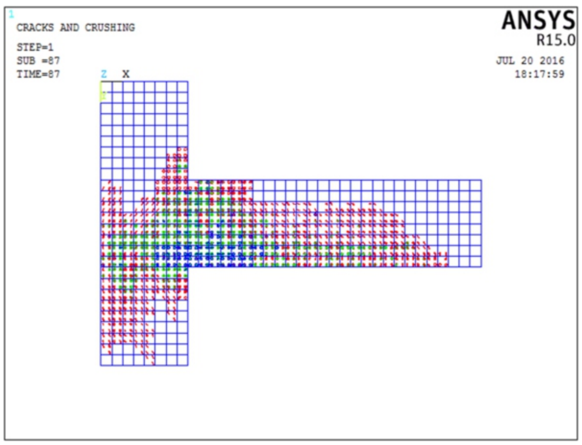

Fig. 15. Control BCJ crack pattern without CFRP

Deflected shape and cracking pattern for specimen repaired with configuration-1 are shown in Figure 16 and 17, respectively.

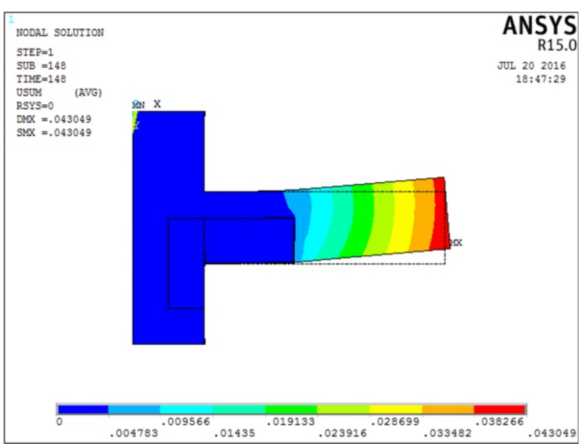

Fig. 16.Repaired BCJ deflection with CFRP configuration-1

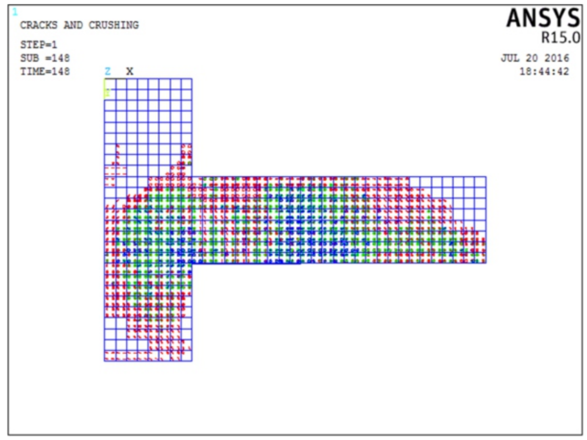

Fig. 17.Repaired BCJ crack pattern with CFRP configuration-1Specimen repaired with

configuration-2 with CFPR and cracking pattern are shown in Fig. 18 and 19, respectively.

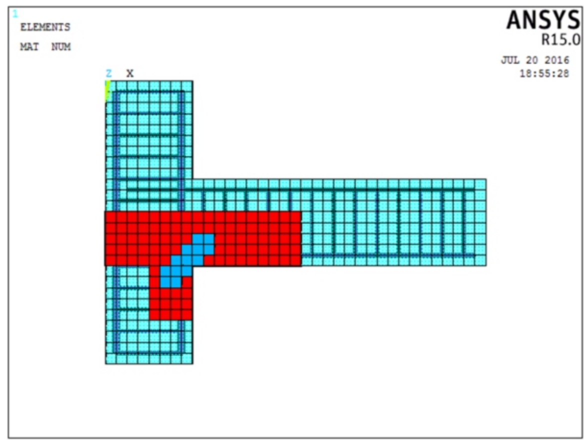

Fig. 18. Repaired BCJ with CFRP config. -2

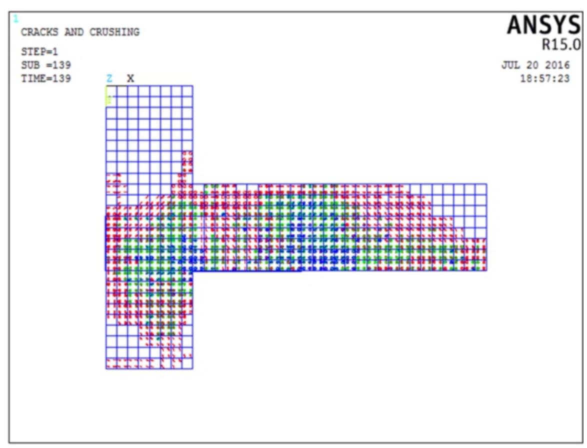

Fig. 19. Repaired BCJ crack pattern with CFRP configuration-2

V. CONCLUSIONS

Energy dissipation capacities were evaluated for the beam column joint specimens repaired with two different types of CFRP configurations. The specimens were also modelled in ANSYS for confirmation of experimental work. It was concluded that, CFRP can be employed to improve the energy dissipation capacity, and load carrying capacity of beam column joints. CFRP wraps shifted the cracks locations away from column face. Experimental results also revealed that stiffness of members cannot be improved by just repairing the cracked specimens using CFRP. Conclusions can be summarized as below:

1. Arrangements of CFRP wrap can affect the Energy dissipation capacity of T joints. As in this research the improvement in relative energy dissipation capacity of CFRP configuration-2 was 25.43 percent higher than configuration 1.
2. There was only 5.25 percent improvement in cumulative energy dissipation capacities of CFRP repaired specimens.
3. Improvement in Energy dissipation capacities also depend on the extent of fracture occurred during first phase of testing. In this research both types of configurations were employed carefully however performance of specimens in terms of energy dissipation observed to be depended on the degree of fracture prior to repair.

REFERENCE

[i] M. H. Mahmoud, H. M. Afefy, N. M. Kassem, and T. M. Fawzy, "Strengthening of defected beam-column joints using CFRP," Journal of advanced research, vol.5, no. 1, pp. 67-77, 2014.

[ii] C. P. Antonopoulos and T. C. Triantafillou, "Experimental investigation of FRP strengthened RC beam-column joints,"Journal of composites for construction, vol. 7, no. 1, pp. 39-49, 2003.

[iii] M. Engindeniz, L. F. Kahn, and Z. Abdul Hamid, "Repair and strengthening of reinforced concrete beam-column joints: State of the art,"ACI structural journal, vol.102, no. 2, p. 1, 2005.

[iv] N. Attari, S. Amziane, and M. Chemrouk, "Flexural strengthening of concrete beams using CFRP, GFRP and hybrid FRP sheets,"Construction and Building Materials, vol. 37, pp. 746-757, 2012.

[v] Q.U.Z. Khan, M. Fiaz Tahir, A. Ahmad, and M. Iqbal, "Seismic Evaluation of Repaired and Retrofitted Circular Bridge Piers of Low Strength Concrete," Arabian Journal for Science & Engineering, vol. 40, no. 11, 2015.

[vi] C. Pantelides, I. Gergely, L. Reaveley, and R. Nuismer, "Rehabilitation of cap beam-column joints with carbon fiber jackets," in Proc., 3rd Int. Symposium on Non-Metallic (FRP) Reinforcement for Concrete Structures, 1997, pp. 587-595.

[vii] K. Soudki, A. K. El-Sayed, and T. Vanzwol, "Strengthening of concrete slab-column connections using CFRP strips," Journal of King Saud University-Engineering Sciences, vol. 24, no. 1, pp. 25-33, 2012.

[viii] M. F. Tahir, "Response of Seismically Detailed Beam Column Joints Repaired with CFRP Under Cyclic Loading," Arabian Journal for Science and Engineering, vol. 41, no. 4, pp. 1355-1362, 2016.

[ix] H. Sezen, "Repair and strengthening of reinforced concrete beam-column joints with fiber-reinforced polymer composites," Journal of Composites for Construction, vol. 16, no. 5, pp. 499-506, 2012.

[x] A. Tsonos and K. Stylianidis, "Pre-seismic and post-seismic strengthening of reinforced concrete structural subassemblages using composite materials (FRP)," in Proc., 13th Hellenic Concrete Conf, 1999, vol. 1, pp. 455-466.

[xi] C. G. Karayannis and G. M. Sirkelis, "Strengthening and rehabilitation of RC beam-column joints using carbon-FRP jacketing and epoxy resin injection," Earthquake Engineering & Structural Dynamics, vol. 37, no. 5, pp. 769-790, 2008.

[xii] Y. A. Al-Salloum and T. H. Almusallam, "Seismic response of interior RC beam-column joints upgraded with FRP sheets. I: Experimental study," Journal of Composites for Construction, vol. 11, no. 6, pp. 575-589, 2007.

[xiii] S. H. Alsayed, T. H. Almusallam, Y. A. Al-Salloum, and N. A. Siddiqui, "Seismic rehabilitation of corner RC beam-column joints using CFRP composites," Journal of Composites for Construction, vol. 14, no. 6, pp. 681-692, 2010.

[xiv] U. Akguzel and S. Pampanin, "Assessment and design procedure for the seismic retrofit of reinforced concrete beam-column joints using FRP composite materials," Journal of Composites for Construction, vol. 16, no. 1, pp. 21-34, 2012.

[xv] S. M. Alcocer and J. O. Jirsa, "Strength of reinforced concrete frame connections rehabilitated by jacketing," ACI Structural Journal, vol. 90, no. 3, 1993.

[xvi] P. Léger and S. Dussault, "Seismic-energy dissipation in MDOF structures," Journal of Structural Engineering, vol. 118, no. 5, pp. 1251-1269, 1992.

[xvii] H. Kuwamura and T. V. Galambos, "Earthquake load for structural reliability,"

Journal of Structural Engineering, vol. 115, no. 6, pp. 1446-1462, 1989.

[xviii] G. Housner and P. Jennings, "The capacity of extreme earthquake motions to damage structures," Structural and geotechnical mechanics, pp. 102-116, 1977.

[xix] E. Martinez-Romero, "Experiences on the use of supplementary energy dissipators on building structures," Earthquake Spectra, vol. 9, no. 3, pp. 581-625, 1993.

[xx] J. Nzabonimpa, W.-K. Hong, and J. Kim, "Experimental and non-linear numerical investigation of the novel detachable mechanical joints with laminated plates for composite precast beam-column joint," Composite Structures, vol. 185, pp. 286-303, 2018.

[xxi] F. Mazza, "Shear modelling of the beam-column joint in the nonlinear static analysis of rc framed structures retrofitted with damped braces," Bulletin of Earthquake Engineering, vol. 16, no. 5, pp. 2043-2066, 2018.

[xxii] ACI Committee, "American Concrete Institute and International Organization for Standardization (2008)," Building code requirements for structural concrete (ACI 318-08) and commentary, 2008.

[xxiii] ACI Committee 315, M. P. S.-. Farmington Hills, American Concrete Institute 2004.

[xxiv] P. Desayi and S. Krishnan, "Equation for the stress-strain curve of concrete," in Journal Proceedings, 1964, vol. 61, no. 3, pp. 345-350.

[xxv] S. P. Timoshenko and J. M. Gere, "Theory of elastic stability. Courier Corporation," 2009.

[xxvi] D. I. Kachlakev, T. Miller, S. Yim, K. Chansawat, and T. Potisuk, "Finite element modeling of concrete structures strengthened with FRP laminates," Oregon Department of Transportation, Research Group 2001.